

AD-A119 912

NAVAL RESEARCH LAB WASHINGTON DC
FURTHER TRIALS OF A STRAIN HARDENING INDEX OF FATIGUE DAMAGE.(U)
SEP 82 J M KRAFFT
NRL-MR-4922

F/6 11/6

UNCLASSIFIED

NL

10-1
40 3
11 3 11 2



END
DATE
FILMED
11-82
DTIC

AD A119912

REPORT DOCUMENTATION PAGE		READ INSTRUCTIONS BEFORE COMPLETING FORM
1. REPORT NUMBER NRL Memorandum Report 4922	2. GOVT ACCESSION NO. AD-A119 912	3. RECIPIENT'S CATALOG NUMBER
4. TITLE (and Subtitle) FURTHER TRIALS OF A STRAIN HARDENING INDEX OF FATIGUE DAMAGE	5. TYPE OF REPORT & PERIOD COVERED Final report	
	6. PERFORMING ORG. REPORT NUMBER	
7. AUTHOR(s) J. M. Krafft	8. CONTRACT OR GRANT NUMBER(s)	
9. PERFORMING ORGANIZATION NAME AND ADDRESS Naval Research Laboratory Washington, DC 20375	10. PROGRAM ELEMENT, PROJECT, TASK AREA & WORK UNIT NUMBERS PR 023-05-45; 58-1502-0-2; WR 022-01-01; 58-0264-0-1	
11. CONTROLLING OFFICE NAME AND ADDRESS	12. REPORT DATE September 28, 1982	
	13. NUMBER OF PAGES 21	
14. MONITORING AGENCY NAME & ADDRESS (if different from Controlling Office)	15. SECURITY CLASS. (of this report) UNCLASSIFIED	
	15a. DECLASSIFICATION/DOWNGRADING SCHEDULE	
16. DISTRIBUTION STATEMENT (of this Report) Approved for public release; distribution unlimited.		
17. DISTRIBUTION STATEMENT (of the abstract entered in Block 20, if different from Report)		
18. SUPPLEMENTARY NOTES		
19. KEY WORDS (Continue on reverse side if necessary and identify by block number) Low cycle fatigue Titanium alloys, fatigue Cyclic stress strain Structural steel, fatigue		
20. ABSTRACT (Continue on reverse side if necessary and identify by block number) -Previous cyclic-strain, smooth-specimen fatigue tests of α - β titanium alloys displayed an anomalous endurance enhancement for some of the alloy conditions. This could be explained by associating resistance to fatigue damage directly with the stress-normalized plastic strain hardening rate at the point of maximum cyclic tensile stress. Since this rate also controls the extent of stress-relaxation-induced tensile creep strain in each cycle, (Continues)		

20. ABSTRACT (Continued)

it was thought that fatigue damage might be associated with it. To test this hypothesis, data with varied load hold time, and over a full range of cyclic life, is reported here for some of the previously reported alloys of Ti-6Al-4V, as well as for an A36 steel plate. Notch fatigue tests of the A36, combined with those of Yoder et al for the titanium alloys, are compared to the smooth specimen data. Results tend to support the damage-inhibiting role of the plastic strain hardening rate, but not of the creep strain portion of each cycle. Notch fatigue data agrees with smooth specimen trends if Neuber's rule is used to characterize the stress concentration factor, particularly with the A36 steel. As with Yoder's notch fatigue results smooth specimen LCF life, though quite different in the range less than 10^3 cycles, tends to converge near the endurance limit, thus mitigating adverse effects of alloy conditions which favor resistance to fatigue crack propagation in α - β titanium alloys.

CONTENTS

NOMENCLATURE iv

INTRODUCTION 1

TEST MATERIALS AND PROCEDURES 2

PROCESSING CYCLIC CURVES FOR L-FACTORS 4

RESULTS ON A-36 STEEL 4

TITANIUM 6Al-4V RESULTS 5

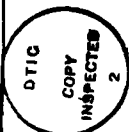
DISCUSSION 6

CONCLUSIONS 7

ACKNOWLEDGMENTS 7

REFERENCES 16

Accession For	
NTIS GRA&I	<input checked="" type="checkbox"/>
DTIC TAB	<input type="checkbox"/>
Unannounced	<input type="checkbox"/>
Justification	
By _____	
Distribution/	
Availability Codes	
Dist	Avail and/or Special
A	



NOMENCLATURE

A	Crosssectional area of specimen
A _o	Initial area of specimen
e	Engineering strain $\Delta l/l_o$
e _p	Engineering plastic strain
E	Young's modulus of elasticity, monotonic
K _f	Fatigue notch factor
K _t	Elastic stress concentration factor
ΔK	Crack tip stress intensity factor excursion
L	A low cycle fatigue factor
N	Cumulative number of complete load/strain cycles
N _f	Cycles to failure by macro-crack initiation
N _i	Cycles to micro-crack initiation
NOD	Notch opening displacement
P	Axial load
S	Engineering stress, P/A _o
S _{max}	Maximum stress of cycle
S _{min}	Minimum stress of cycle
R	S _{min} /S _{max}
e	Total true strain
e _p	True plastic strain
ρ	Notch root radius
σ	True stress, P/A
σ _{max}	Maximum notch stress
Δ	Total excursion in one cycle
θ _t	Tensile tangent modulus dS/de
θ _{to}	Elastic tensile tangent modulus
θ _o	Elastic true strain hardening rate
θ _{tp}	Plastic tensile tangent modulus
θ	True strain hardening rate dσ/de
θ _p	True plastic strain hardening rate

FURTHER TRIALS OF A STRAIN HARDENING INDEX OF FATIGUE DAMAGE

INTRODUCTION

This study is part of an NRL program probing influences of microstructural variables on the fatigue endurance of α - β titanium alloys. Fatigue is important in naval aircraft where it often limits the safe life of jet engine components. Reported in earlier papers, Yoder, Cooley and Crooker [1, 2] have identified large beneficial reductions of fatigue crack growth rate with increased grain size, such as obtained by annealing at near or above the beta transus temperature. Consequence of such treatments in terms of fatigue crack initiation, the primary event in failure of jet engine components, is yet of concern. To assess this, low cycle fatigue (LCF) crack initiation from smooth specimens has been studied by this writer [3] while from notched ones by Yoder et al [4]. Intercomparison of the two kinds of fatigue data was postponed, however, since the ranges of cyclic life scarcely overlapped. Present smooth-specimen data provides such overlap, so a comparison is attempted here.

The enlarged data base on cyclic strain fatigue of smooth specimens is of some interest in itself. For it permits a more critical test of a damage algorithm devised for the earlier data in the cyclic life range of less than 10^3 [3]. Here, some heat treatment conditions of Ti-6Al-4V, as well as of Ti-8Al-1Mo-1V, showed an unusual endurance pattern. Relative to the normal straight-line Coffin relationship between log endurance and log plastic strain excursion, some materials exhibited a distinct rightward shift of points in the 10 - 100 cycle fatigue life range. It was noticed that materials which show this effect also exhibit a transient development in the form of the cyclic stress-strain curve. Termed "inverted strain hardening", what appears as ordinary cyclic softening in the first half of each excursion is reversed by extra strain hardening in the latter half, restoring the peak stress to its normal level. In extreme cases, this effect results in a complete reversal in the normal decline of strain hardening rate with strain, producing a concave rather than convex-upward tensile stress-strain curve. Clearly, the extra endurance could be associated with extra strain hardening rate in the peak stress regions of the hysteresis loop. A direct correspondence between the two behaviors was achieved by associating resistance to initiation damage with the stress-normalized rate of plastic-strain hardening. A factor L, which is proportional to the initiation life N_i , was defined as

$$L \equiv \left(\frac{\sigma_p}{\Delta\sigma/2} - 1 \right)^* \approx \frac{\sigma_p}{\Delta S/2} \sim N_i \quad (1)$$

Indeed plots of the L factor as a function of the plastic strain excursion corresponded nicely with the trends in fatigue endurance, including the curious low-life-range endurance enhancements. This seemed useful as the proportionality factor

*The earlier work used $\sqrt{3}/2$ vs present simpler 1.0 for this constant, a minor change.

N_i/L provided a single-parameter characterization of an entire LCF behavioral pattern. But whether applicable over a full range of LCF life could not be determined with the limited range of earlier data.

Evidence for the N_i to L connection being only circumstantial, a rationale was sought. The rate of plastic-strain hardening is inversely related to the transient creep strain in each cycle, simply inversely proportional in an algorithm used in fatigue crack propagation modeling [5]. Strain range partitioning studies of Manson, Halford and associates [6] often show the least endurance when tensile straining is exclusively of constant-load creep. But whether such damage could dominate in these alloys at ambient temperature was unresolved by the earlier data collection. The new data probes this question too.

TEST MATERIALS AND PROCEDURES

Titanium alloys of this study are of the Ti-6Al-4V system. Originally, four 25.4 mm (1.0 inch) plates were purchased with differing levels of interstitial oxygen. The new data has been gathered on three of these, all but that of 0.11 oxygen. Chemical analysis, heat treatment schedules and resulting mechanical properties are listed in tables I, II and III respectively, including the 0.11 oxygen material.

At this (late) stage in our overall titanium program, available stocks of specimen material and the cost of preparing specimens limited the number of specimens available for this study. A good number of mild steel specimens remained from an earlier study by Stonesifer and author [7], so these were used to develop techniques and probe hold time effects, despite the extreme differences between A36 and the titanium alloys. The specimens of A36 steel were obtained from a 25.4mm (1.0 inch) thick plate, and chemical analysis showed it to meet the requirements for ASTM A283 Grade C: C 0.17%, Mn 0.86, P 0.015, S 0.021, Si 0.29, Cu 0.03, O 0.065, H 0.005. Tensile properties are also within this specification: lower yield strength 0.256 GPa (37ksi), ultimate tensile strength 0.456 (66ksi), reduction in area 59%, and elongation at rupture 30% in a gage length of four diameters (2 inches). No extra heat treatment was given the plate, and the uniformity of data from various specimens indicate none was necessary.

The two types of specimen, smooth and notched, are shown in Fig. 1. The notch fatigue specimen is the 1T-CTS of ASTM test method E647-78T. The smooth round specimen is scaled to a size which permits broken halves of the 1T-CTS to be used as specimen stock. Both titanium and steel specimens were tested in long transverse orientation (TL). The smooth specimens were finished with a fine lathe cut and then smoothed rotationally with #400 grit abrasive paper. Trials on effects of surface finish showed this preparation to suffice. The A36 notches were smoothed by a

final cut with a straight fluted reamer, and although some circumferential machining marks remained they did not appear to act as crack starters. This is consistent with results of May et al [8] who find no sensitivity to notch smoothness over the range of surface finish from 2 to 30 micro inch. The excursion in maximum stress at the notch root is calculated from the crack tip stress intensity factor ΔK , as given in ASTM test method E647-78a for this CTS specimen, applied in the manner Barsom and McNicol [9]

$$\Delta\sigma_{\max} = \frac{2\Delta K}{\sqrt{\pi p}} \quad (2)$$

The cyclic frequency limitation in earlier tests performed in a mechanical INSTRON machine was increased by the availability of a more modern electro-hydraulic servo-control machine of the same manufacturer. It was augmented by a programmable MTS function generator, allowing hold time after ramp loading to be varied at will. An alignment subpress, described earlier [3], was used for the smooth specimen tests. Longitudinal strain on the titanium alloys was detected with an opposed-contact, four-finger strain gage. However on the A36 steel, cracks tended to initiate in the finger contact regions, so a two-lobed diametral gage of low contact pressure was used instead. Conventional X-Y recording, pen chart as well as oscilloscopic, was complemented by a digital peak signal indicator. With the notched CTS type specimen, a standard ASTM E399 type clip gage detected displacement at the mouth of the notch slot.

Since load hold time effects are sought, most of the tests were run in the load-control mode. Wave forms for the notch fatigue loading was sinusoidal, while a trapezoid form, with hold to (tensile) loading time ratios of 0.1 and 1.0 generally, was used for the smooth specimens. The cyclic frequency for each test was selected to minimize test duration while assuring fidelity of loading pattern and recording, generally in the range 0.1 to 3 Hz. A load ratio R of 0.1 was maintained.

Crack initiation was detected both mechanically and visually. A plot of minimum and excursion values of notch opening displacement is shown in Fig. 2, where the points of macro-crack initiation are marked. On the smooth specimen tests, load excursion and mean load was manually adjusted in order to maintain the excursion and mean level of strain constant. After cyclic equilibrium is reached, little adjustment is required until crack initiation, after which it must be decreased regularly. With such a small test section, crack initiation and final failure are relatively close together, so the figures in this paper show only the latter, conservative values of N_i designated as cycles to crack, N_f .

PROCESSING CYCLIC CURVES FOR L-FACTORS

L-factor values may be obtained from the cyclic stress strain curve of each test, or alternatively from a single test of full cyclic excursion. In the individual tests of differing strain excursion, values of stress excursion and tangent modulus at the extreme of tensile loading are measured relative to the plastic strain excursion to that point. A corresponding set of values on the full cyclic curve is taken on it at the same value of plastic strain excursion, with stress excursion measured from the compressive toe to that point. The latter procedure is illustrated in the right hand insert of Fig. 3 for a full cyclic test of A36 steel. Measured values are "trued" by usual conversion formulas such as given in Ref. [10]. Plastic values of strain hardening rate are found by subtracting the specific value of true elastic compliance which is measured in that test. Values of L using the measured tensile values directly, shown as the alternative form of Eq (1), agree closely, as shown in the upper block of Fig. 3.

The lower block of Fig. 3 shows these L-values in a logarithmic plot against total strain excursion. Throughout this paper, the elastic part of total strain is based on (the measured value of) the monotonic Young's modulus E, Table III, which is usually somewhat greater than the cyclic value. The scatter in L values from different tests is usually quite low, although some differences could be associated with different heat treatment batches of the titanium alloys.

RESULTS ON A-36 STEEL

The amount of stress-relaxation-induced creep strain was varied by using different hold time relative to a loading time (t_H/t_L) in a trapezoidal wave form, as noted earlier. From results on the A36 steel, Fig. 4 shows both the total plastic strain excursion and the tensile creep portion of this vs cycles to crack N_f . If the creep strain were in control of damage, both hold time ratios would form a single data trend. Obviously they are separated, whereas the total plastic strain range does merge data of the two hold-time ratios. The same result is found in the titanium alloys, although once this became evident, hold time was eliminated as a systematic test variable.

In view of the "non-effect" of hold time, subsequent data plots are referred to the total strain excursion. This facilitates comparison with notch fatigue data, and also provide a definite measurement near the LCF endurance limit where the plastic strain range becomes too small for accurate measurement. Fig. 5 shows the A36 data of Fig. 4 plotted vs the total strain excursion. The curve through the data (upper plot) is transferred from the plot of L values in Fig. 3. A reasonable degree of correspondence is found, with a location at N_f/L ($=N_i/L$) of about 150, a value high relative to those typical of high strength titanium alloys as listed in Table III. The notch

fatigue data is shown on Fig. 5 as an elastic strain excursion, equivalent to the Eq (2)-calculated stress excursion value relative to the monotonic value of Young's modulus. The trend in notch stress data is consistent with data of Novak [11] for A36 steel in salt water when the stress excursion exceeds the endurance limit of the air environment. However, the notch-stress points fall below the smooth specimen results as the strain excursion increases.

The divergence of notch vs smooth specimen strain excursion for given endurance is a problem of long standing [12]. It is often characterized by a variable fatigue stress concentration factor K_f . Use of Neuber's rule [13] often reduces or even removes the variability in K_f . A form of this rule suggested by Topper, Wetzell and Morrow [14] is to compare the elastic-calculated values of notch strain with the geometric mean of individual values of smooth specimen elastic strain and total strain excursion. This is done in the lower part of Fig. 5 where each of the small circles corresponds to an to an upper large circle but plotted vs $\sqrt{\Delta\epsilon \Delta\sigma/E}$ rather than vs $\Delta\epsilon$ alone. With this, the agreement of smooth with notched specimen data is better. It could be further improved by a slight change (increase) in the value of K_f , taken here as equivalent to K_t . Recent work of Soanouni and Bathias [15] provides a systematic way of making this adjustment in K_f . The dashed curve was obtained by graphically fitting the sets of L-values from Fig. 3 after plotting them vs the Neuber strain equivalent.

TITANIUM 6Al-4V RESULTS

Results of the smooth specimen LCF tests on titanium alloys are presented in the same format as Fig. 5 for the A36. Fig. 6 shows data for the 0.20% oxygen material in recrystallization anneal (RA) condition. All of the data points beyond 10^3 cycles are new, while those below comprise also those reported in reference [3]. The new vs old data points are not coded as they were found to merge into the same data trend. Conversion to Neuber strain drops the position of data points significantly only for $\Delta\epsilon$ values above about 1.5%. Below this, the shift is negligible and the single data point covers both positions. The notched (CT) specimen results appear to parallel the smooth specimen data but lie some 20% higher, suggesting a (strain based) K_f of about 80% of K_t for this material. Notch radius and R-value may also affect the value of K_f which present results do not address, although present notch radius, 1.6 mm, is thought to be in a range of low sensitivity to notch radius. Both the current A36 specimens and those used by Yoder et al for Ti alloys employed a 1.6 mm notch radius.

The L-factor curves for the titanium alloys are branched to show maximum allowance for the "inverted strain hardening" effect. The prior work [3] showed that this can be done by increasing the early-life values of plastic strain hardening rate by a constant increment, $\Delta\theta$, independent of the strain excursion. This extreme value of L is calculated then as

$$L = [(\theta_p + \Delta\theta)/2\Delta\sigma - 1] \quad (3)$$

Values of $\Delta\theta$ are taken from Ref. (3) as listed in Table III. As the value of θ_p increases, the $\Delta\theta$ change becomes relatively small and the branch^p merges with the basic L-trend. Experience shows the actual data to follow the right hand branch for a while but at very high-strain, low-life, to cross over to the normal curve since here failure occurs before the strain hardening in tension is completed. In Fig. 6, the L-curves fit well in the range below 10^3 cycles but ride about 20-30% above the smooth specimen data in the range beyond.

Results on the 0.18% oxygen material in beta anneal (3A) condition are shown in Fig. 7. Here the L-curve fits the smooth specimen data nicely. Notch data above the endurance limit was not available on this material, but what is present suggests a value of K_f close to K_t .

The 0.06 oxygen plate BA material, Fig. 8, has one notch fatigue data point in the endurance range around 10^3 , and four beyond 10^5 . Agreement between the two data sets is good, and a K_f slightly greater than K_t is indicated.

Yoder et al have collected notch fatigue data on two other conditions of the 0.20% oxygen plate: its as-received mill anneal condition, MA and after a beta anneal in NRL facilities, BA. These are shown in Figs. 9 and 10 respectively, as compared to the smooth specimen LCF data and L factor curves developed earlier [3]. Agreement seems good but the lack of new smooth specimen data beyond 10^3 cycles prevents critical comparison.

DISCUSSION

A stated objective of this program was to assess losses in LCF endurance relative to gains in propagation resistance. One way of ranking smooth specimen performance is through the L-curve fitting constant N_f/L ($\approx N_i/L$). The values used here are essentially as found in the earlier study of these materials as listed in Table III; they range from 3 to 8. A36 by way of contrast has a value more than 10x that of any of the titanium alloys: 150. Actual rankings depend to some extent on the manner of presenting the data and the strain-range of interest. Since design allowables are generally based on a stress criteria, such a format is used in Fig. 11 for the three conditions of Ti-6Al-4V for which a complete range of data is available. This combines the total strain excursion plots of Figs. 6, 7, & 8 but normalized to individual values of E from Table III. Here in the

low life end, the ordering is pretty much as indicated by the ranking of L parameter fitting factors. However, for endurance greater than 10^3 cycles, the range of usual engineering importance, the data merges together into a single scatter band. This is not to say that differences may not occur at greater cyclic life. But it does say that gains in propagation resistance need not necessarily incur a penalty in initiation life. Both kinds of data are needed to make an assessment. The notch fatigue data taken together has led Yoder et al [4] to the same conclusion.

CONCLUSIONS

From this extension of Ti-6AL-4V smooth specimen LCF data into the 10^3 to 10^5 cycle range, with supplementary smooth and notch-specimen data on A36 steel, the following conclusions are drawn:

1. Crack initiation life at room temperature in these materials is little affected by load hold time, and corresponding stress-relaxation-induced creep, except to the extent that this contributes to the total plastic strain excursion, with which the endurance correlates closely. This result eliminates the creep damage criterion as a possible explanation for an observed correlation of initiation endurance with stress normalized plastic strain hardening rate.

2. The L-factor of stress normalized plastic strain hardening rate correlates the extended LCF data sets fairly well. Further trials are needed to establish its utility as a predictive tool, however.

3. Notch fatigue initiation data based on the ΔK -derived elastic strain correlates with smooth specimen data relative to total strain excursion in the region of small plastic strain excursion. However, the data on mild steel shows a marked divergence with increased plastic strain excursion. Comparing the data using a Topper et al adaptation of Neuber's rule brings the data into much closer agreement, and a constant near- K_t value of K_f provides a close correspondence of the two kinds of data.

4. In the LCF endurance range below 10^3 cycles, increases in grain size or of interstitial oxygen content appear detrimental to strain based initiation endurance in Ti-6AL-4V. However, in the range above, little difference is observed. This result is consistent with that of Yoder et al derived from notch fatigue data on these same materials.

ACKNOWLEDGMENT

Author is indebted to Dr. George R. Yoder for generous assistance in matters metallurgical, and especially for permission to show his yet to be published notch fatigue data in Figures 7 and 8 of this paper.

Table I — Chemical analyses

Alloy	Content (wt-%)								
	O	Al	Mo	V	Fe	N	C	H	Al*
Ti-6-4	0.06	6.0	—	4.1	0.05	0.008	0.023	0.0050	7.0
Ti-6-4	0.11	6.1	—	4.0	0.18	0.009	0.02	0.0069	7.6
Ti-6-4	0.18	6.6	—	4.4	0.20	0.014	0.02	0.0058	8.9
Ti-6-4	0.20	6.7	—	4.3	0.10	0.011	0.03	0.0060	9.2

Note: Al* is the aluminum equivalent

$$Al^* = Al + \frac{Sn}{3} + \frac{Zr}{3} + 10(O + C + 2N).$$

Table II — Heat treatments for Ti-6Al-4V

Heat Treatment Type	Specification*
MA	788°C, 1 h / AC (as received)
RA	954°C, 4 h/HC @ 180°C/h to 760°C/AC @ 370°C/h to 482°C/AC
BA	1038°C, 0.5 h/HC to RT + 732°C, 2 h/AC

*Anneals performed in vacuum furnace; h = hour, WQ = water quench, FC = furnace cool, HC = cooled in He @ approx. air cooling rate, AC=air cool.

Table III — Mechanical properties

Alloy	Heat Treatment	Orientation	0.2% Yield	Tensile	Young's	Reduction in Area	Elongation*	Effective Grain Size	ISH	N _i		
			Strength	Strength	Modulus							
	Wt-% Oxygen	No	Type	σ_y	σ_{uts}	E	(%)	(%)	\bar{T}	$\Delta\theta$	$\frac{N_i}{L}$	
				(MPa)	(MPa)	(GPa)			(μm)	(GPa)	(cycles)	
Ti-6-4	0.20		MA	T	1007	1034	130	29	14	5	7.6	6.0
Ti-6-4	0.20		RA	T	931	1007	130	26	15	9	6.2	7.0
Ti-6-4	0.20		BA	T	869	958	117	16	11	24	0.3	2.9
Ti-6-4	0.18		BA	T	818	906	120	13	8	38	1.4	3.4
Ti-6-4	0.11		BA	T	772	869	118	19	10	28	2.1	4.4
Ti-6-4	0.06		BA	T	740	818	115	34	10	17	6.2	8.0
Ti-6-4	0.06			L	772	829	115	26	10			

*50.8-mm gage length

NOTCHED CTS

SMOOTH T-C

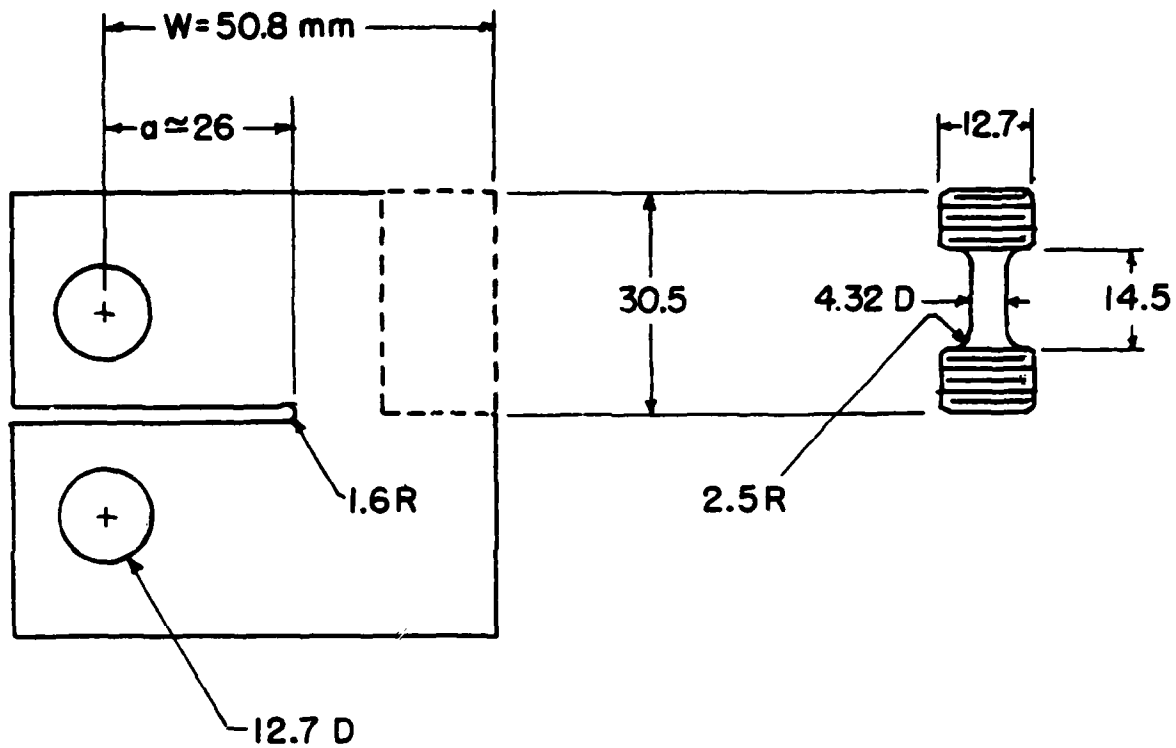


Fig. 1 — Profiles of notch fatigue specimen and subsize smooth tension — compression specimen which can be machined from broken remnants.

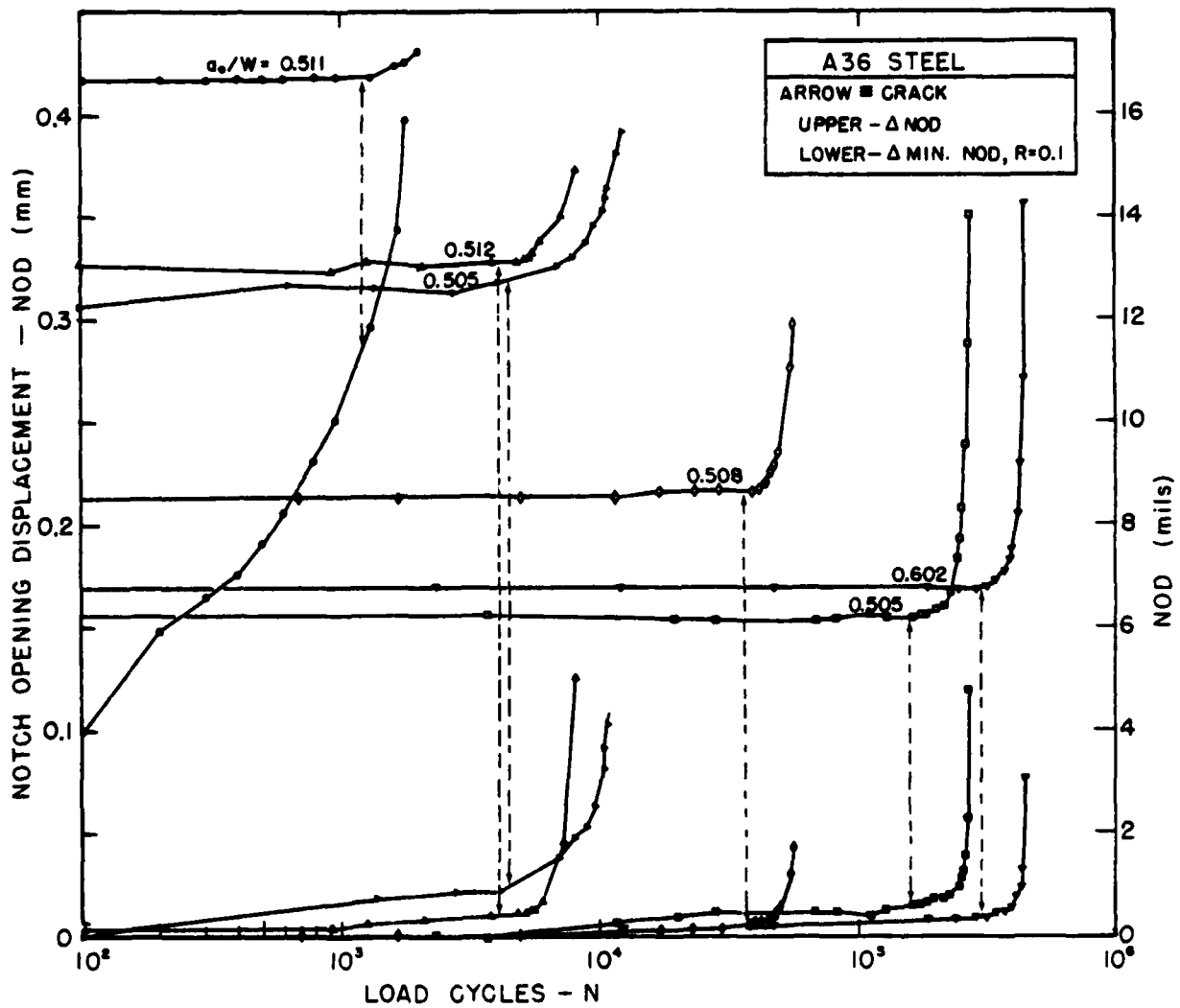


Fig. 2 -- Plot of notch opening excursion and the minimum displacement starting from its initial value, showing a rapid upswing after crack initiation.

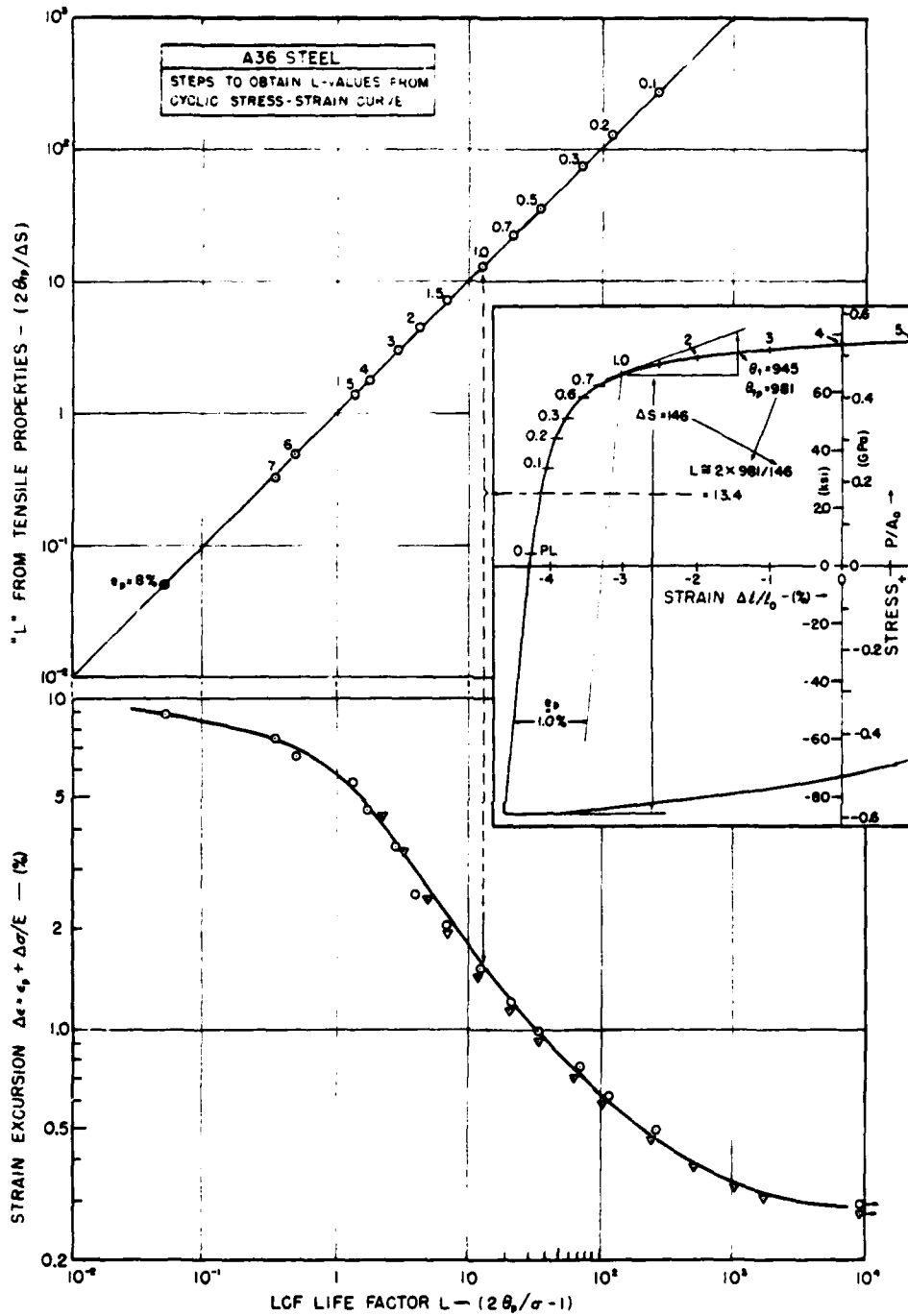


Fig. 3 — Values of nominal stress excursion and tangent modulus at various levels of plastic strain, right center, combine to provide L-values, which may be determined by a simple calculation using tensile properties directly, on upper plot, and displayed vs total strain excursion lower plot, where additional data points are from recording with 2x strain amplification.

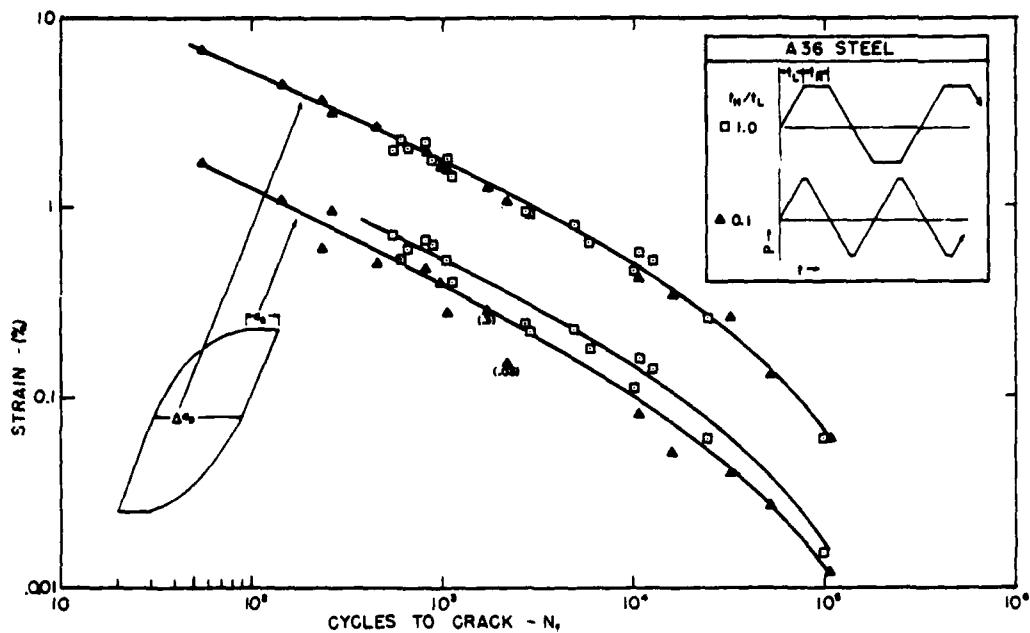


Fig. 4 — In A36 steel, the amount of constant-load creep strain, varied by hold time ratio, affects endurance only as a part of the total plastic strain excursion.

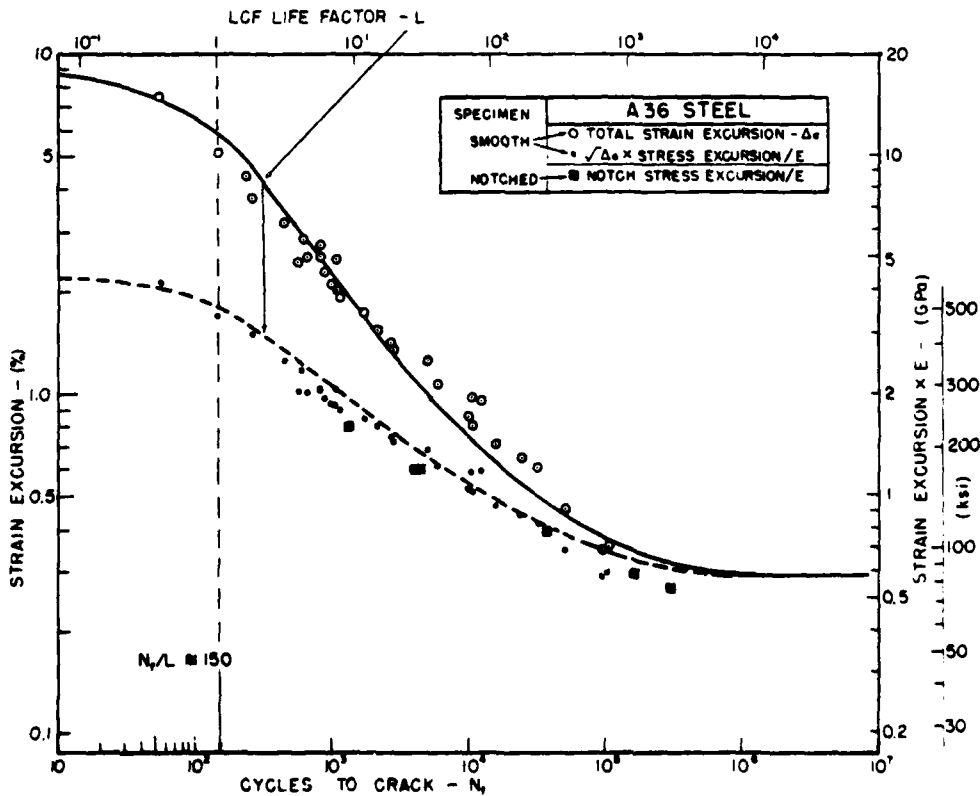


Fig. 5 — LCF smooth specimen endurance of A36 is shown vs total strain excursion above and vs Neuber strain below, which better matches notch fatigue life relative to elastic strain estimates. The curves are L-factor trends from Fig. 4.

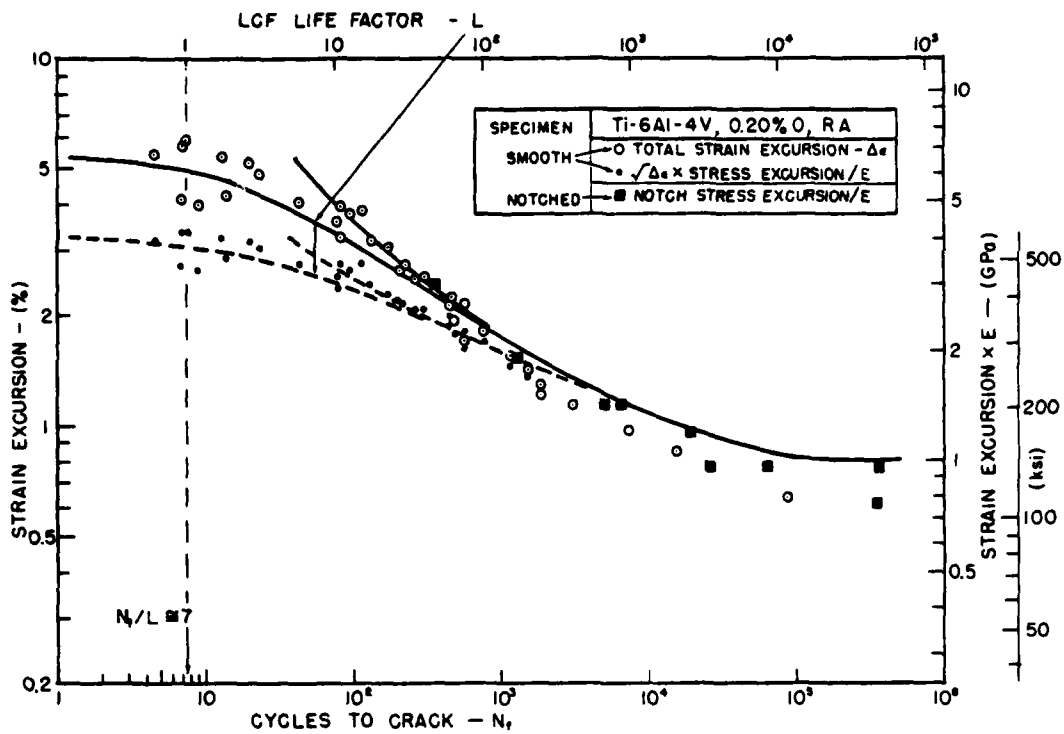


Fig. 6 - Smooth and notch fatigue data on Ti-6Al-4V, 0.20% O, RA, in format of Fig. 5.

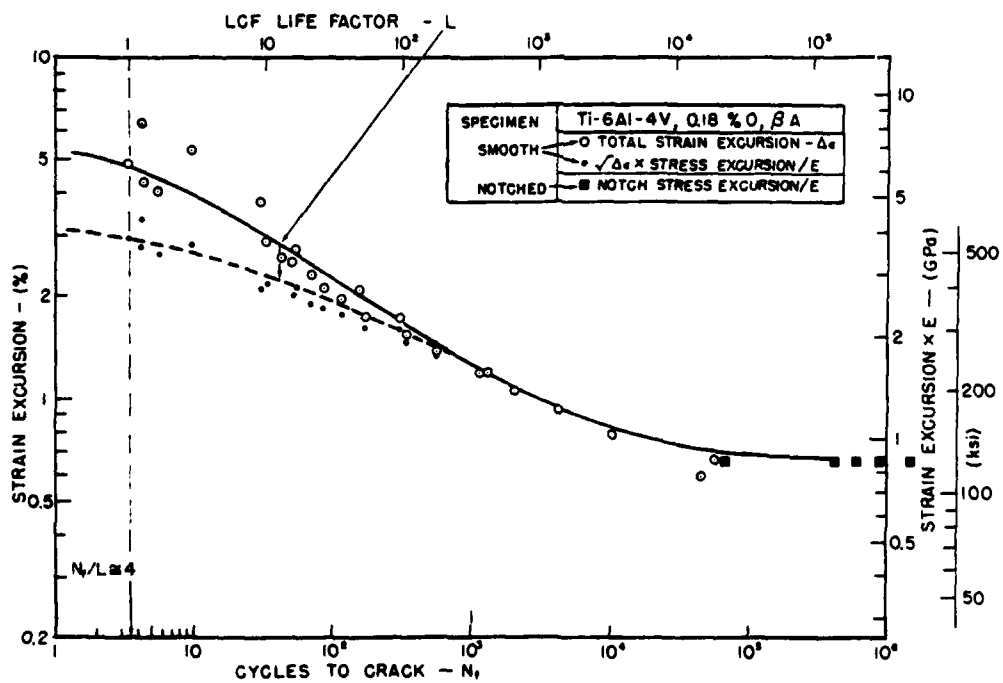


Fig. 7 - Smooth and notch fatigue data on Ti-6Al-4V, 0.18% O, BA, in format of Fig. 5.

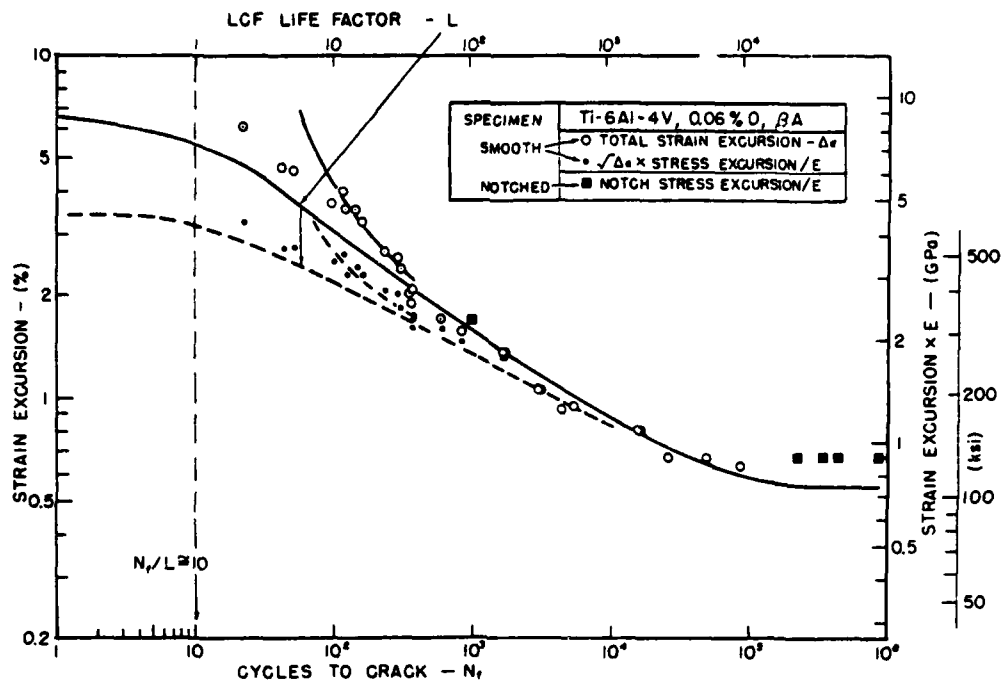


Fig. 8 - Smooth and notch fatigue data on Ti-6Al-4V, 0.06% O, BA, in format of Fig. 5.

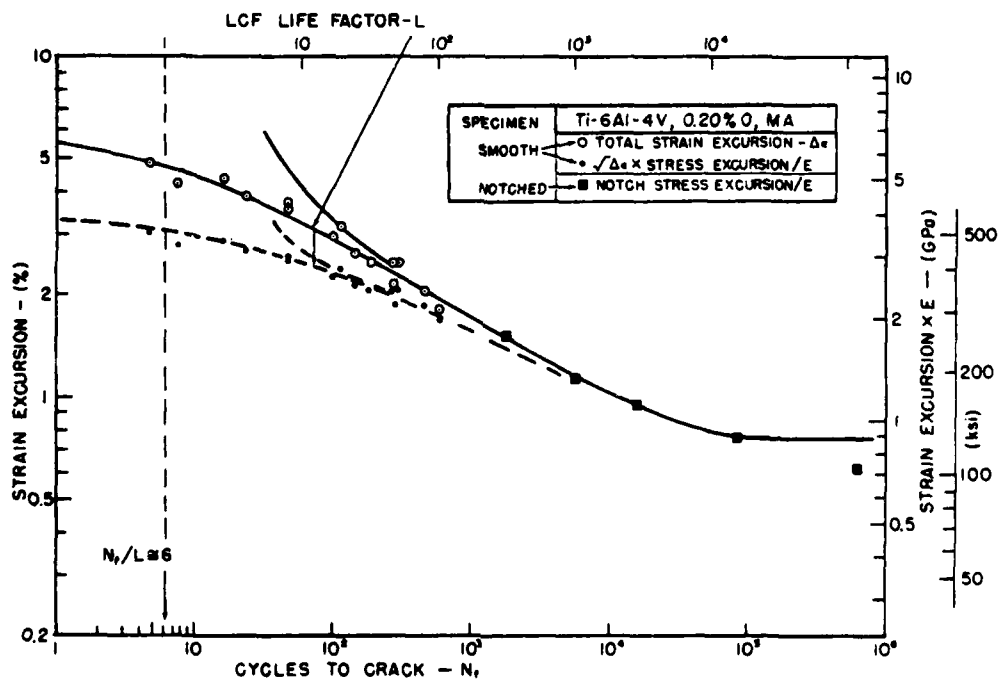


Fig. 9 - Smooth and notch fatigue data on Ti-6Al-4V, 0.20% O, MA, in format of Fig. 5.

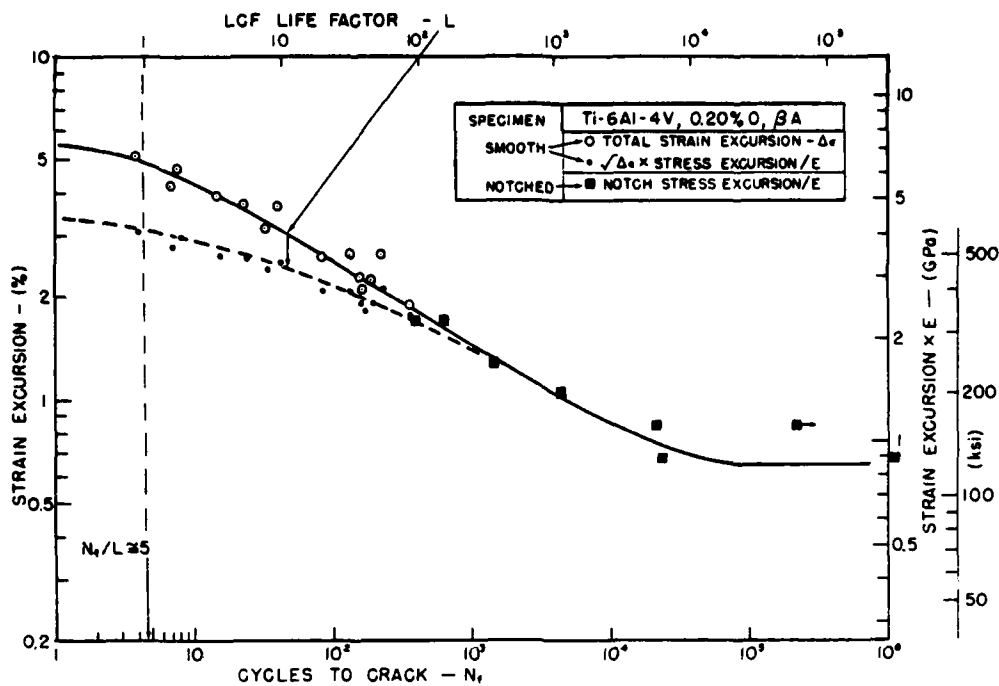


Fig. 10 - Smooth and notch fatigue data on Ti-6Al-4V, 0.20% O, βA, in format of Fig. 5.

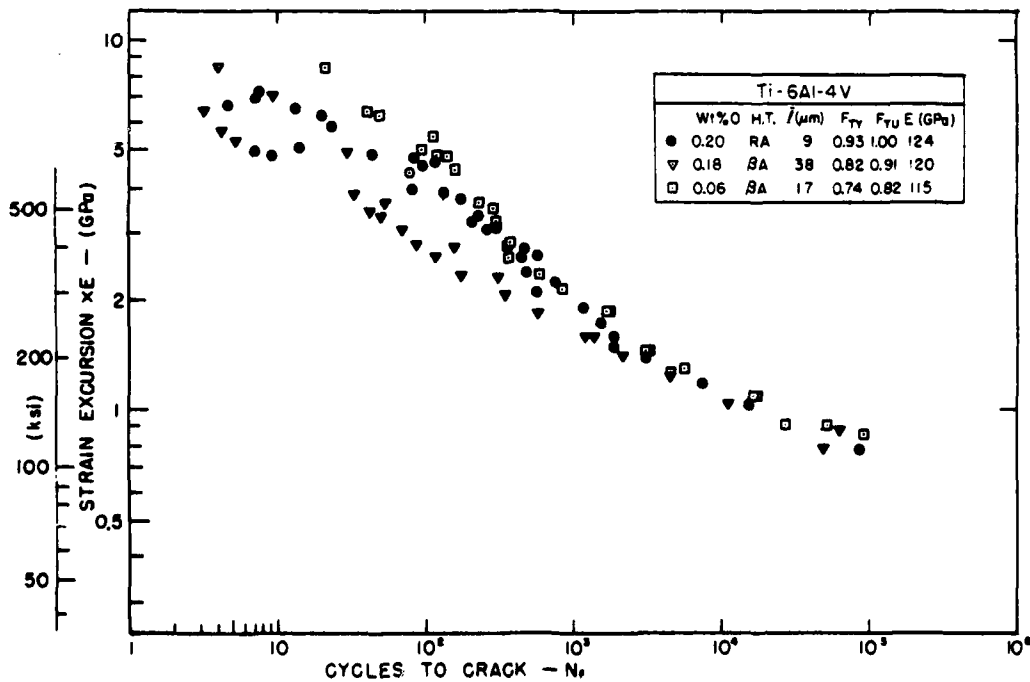


Fig. 11 - Total strain derived stress excursion vs cycles to crack for three conditions of Ti-6Al-4V shows the marked differences at low cyclic life tend to disappear above 10^3 cycle endurance.

REFERENCES

1. G.R. Yoder, L.A. Cooley and T.W. Crooker, "Enhancement of Fatigue Crack Growth and Fracture Resistance in Ti-6Al-4V and Ti-6Al-6V-2Sn Through Microstructural Modification," J. Engineering Materials and Technology, 99, Oct 1977, pp. 313-318.
2. G.R. Yoder, L.A. Cooley and T.W. Crooker, "50-Fold Difference in Region-II Fatigue Crack Propagation Resistance in Titanium Alloys: A Grain Size Effect," J. Engineering Materials and Technology, 101, Jan 1979, pp. 86-90.
3. J.M. Krafft, "Effect of Stress-Strain Behavior on Low-Cycle Fatigue of α - β Titanium Alloys," Fatigue of Engineering Materials and Structures, Vol. 4, 1981, pp. 111-129.
4. G.R. Yoder, L.A. Cooley and T.W. Crooker, "A Comparison of Microstructural Effects on Fatigue-Crack Initiation and Propagation in Ti-6Al-4V," NRL Memorandum Report 4758, Mar. 5, 1982, See also AIAA paper 82-0660-CP, Proc. 23rd Structures, Structural Dynamics and Materials Conference, New Orleans, May 1982, CP823, Pt. 1, pp. 132-136.
5. J.M. Krafft and W.H. Cullen, Jr., "Organizational Scheme for Corrosion-Fatigue Crack Propagation Data," Engineering Fracture Mechanics 10, 1978, pp. 609-650.
6. G.R. Halford, M.H. Hirschberg and S.S. Manson, "Temperature Effects on the Strain Range Partitioning Approach for Creep Fatigue Analysis," ASTM STP 520, 1973, pp. 658-669.
7. F.R. Stonesifer and J.M. Krafft, "Fatigue Crack Growth in A36/A283 Plate in Air and Sea Water Environments," NRL Memorandum Report 4467, March 1981.
8. R.A. May, A. Stuber and S.T. Rolfe, "Effective Utilization of High Yield Strength Steels in Fatigue," WRC Bulletin 243, November 1978, pp. 1-26.
9. J.M. Barsom and R.C. McNicol, "Effect of Stress Concentration on Fatigue Crack Initiation in HY-130 Steel," ASTM STP 559, 1974, pp. 183-204.
10. D.T. Raske and Jo Dean Morrow, "Mechanics of Materials in Low Cycle Fatigue Testing," ASTM STP 465, 1969, pp. 1-25.
11. S.R. Novak, "Corrosion Fatigue Crack-Initiation Behavior of Four Structural Steels," Paper presented at ASTM Symposium on Corrosion Fatigue, St. Louis, MO, Oct 1981, forthcoming in ASTM STP.
12. B.M. Wundt, "Effect of Notches on Low Cycle Fatigue," ASTM STP 490, 1972.

13. H. Neuber, "Theory of Stress Concentration for Shear-Strained Pismatical Bodies with Arbitrary Non-Linear Stress Strain Law Trans., ASME, J. Applied Mechanics, 28,4, Dec 1961, pp. 544-550.

14. T.H. Topper, R.M. Wetzel and JoDean Morrow, "Neuber's Rule Applied to Fatigue of Notched Specimens," Journal of Materials, 4, 1, Mar 1969, pp. 200-209.

15. K. Soanouni and C. Bathias, "Study of Fatigue Crack Initiation in the Vicinity of Notches," Engineering Fracture Mechanics, 16, 5, 1982, pp. 695-706.